RJC

RASĀYAN *J. Chem.*
Vol. 18 | No. 4 |1886-1892| October-December | 2025
ISSN: 0974-1496 | e-ISSN: 0976-0083 | CODEN: RJCABP
http://www.rasayanjournal.com
http://www.rasayanjournal.co.in

CARBON MICROTUBES SYNTHESISED BY AERATION-CONTROLLED PYROLYSIS: PHOTOCATALYTIC AND SURFACE ENERGY INVESTIGATIONS

A. Sunitha[1], K. Chennakesavulu[1,2,✉] and G. Ramanjaneya Reddy[2]
[1]Department of Chemistry, Sathyabama Institute of Science and Technology (Deemed to be a university), Chennai-600119, (Tamil Nadu), India
[2]Center for Nanoscience and Nanotechnology, Sathyabama Institute of Science and Technology (Deemed to be University), Chennai-600119, Tamil), India
✉Corresponding author: chennanml@yahoo.com

ABSTRACT

This article focuses on the streamlined innovation method for the synthesis of carbon microtubes (CMTs) from cotton fibers in an open-air pyrolysis under optimized conditions. The optimized synthesis conditions were achieved by controlling the rolling and combustion dynamics of the cotton fibers, which facilitated the formation of well-defined carbon microtubular structures. The optimized synthesis conditions were achieved by controlling the rolling and combustion dynamics of the cotton fibers, which facilitated the formation of well-defined carbon microtubular structures. The synthesized CMTs were thoroughly investigated by powdered XRD, Contact angle, Raman spectroscopy, FESEM, XPS, N_2-isotherms, BET, and surface energy. The methylene blue (MB) dye removal efficacy was tested for all CMT photocatalysts, The CMT_2 removes best, CMT_3 begins quickly but stops, CMT_1 is medium, and CMT_4 is least effective. Because of its low surface energy (22.1-24.4 mN/m), CMT_2 is hydrophobic. It reacts badly with water but positively with ethanol and n-hexane. CMT_2 is perfect for adsorption in solvents, either non-polar or mildly polar.

Keywords: Surface Energy, CMTs, Differential Aeration, Methylene Blue, SDG6, SDG7

RASĀYAN *J. Chem.*, Vol. 18, No.4, 2025

INTRODUCTION

Fullerenes, CNTs, CMTs, graphite, the porous carbons, diamond, nanospheres, and carbon micro coils develop allotropes.[1-3] However, CNT conflation and advancements are well-studied. CNTs have many advantages; their availability, diameter, quantity, solubility, dispersion in aqueous medium, and mixed solvent systems are difficult for surface energy characteristics wise. Hence, Carbon microtubules cannot be made using arc discharge or pulse laser ablation.[4,5] To overcome CNTs' disadvantages and improve CMTs' benefits, establish physicochemical features.[6] We previously described simple carbon microtube fabrication methods.[6] Carbon microtubes manufactured from willow catkins, kopak fibre, and discarded cotton have been little studied.[7] In recent years, carbon-based material synthesis research groups have grown. This study contributes to Sustainable Development Goals (SDGs) 6 and 7 for clean water and sanitation, affordable and clean energy by enhancing water purification by removing pollutants using CMTs catalytic methods under solar or visible-light photocatalysis for sustainable energy.[8] Roger Bacon of Union Carbide Company reported graphite whiskers from 1800 ºC carbon monoxide pyrolysis in the 1960s.[9] The CMTs are tubular structures with sizes from 5 to 100 µm and was created by carbonizing poly (acrylonitrile) fibres, poly(ethylene terephthalate), catkins, coconut oil, methane, reed bristles, Urea, plant biomass, and PVB powder. And structure makes CMTs strong, ductile, conductive, and low-density.[7-13] CMTs may generate/store energy and serve other large-scale purposes.[12,13] CMTs conducting material production from economically insulting carbon sources is unproven. Carbon-based resorcinol/formaldehyde aerogels displayed Pseudo-second-order kinetics and Freundlich isotherm behavior for methylene blue adsorption. CMTs made from cotton exhibit superior tannic acid adsorption capacity (596.5 mg/g at 1100°C) compared to carbon nanotubes due to π-π interactions and hydrogen bonding, making them more cost-efficient, repeatable, and effective.[14-16] In this study, CMTs are synthesized by pyrolyzing surgical cotton in open air. The first and cheapest way to make carbon microtubules under optimized circumstances. Synthesized

http://doi.org/10.31788/RJC.2025.1849380

CMTs have been examined and their surface energy quantified, which is important in surface chemistry, adsorption, and as anodes in Al/C batteries and super capacitors. We used CMTs to remove MB dye and recorded the percentages under visible light.

EXPERIMENTAL

Materials and Methods

XPS was performed using an Al Kα monochromatic source, XM1000 Omicron equipment in a He-Ne laser, and NANO PHOTON11i. Raman analysis by Rigaku Smart Lab spectra. Powder XRD with Cu Kα radiation (λ = 1.5418 Å) confirmed CMTs' crystalline structure. A Carl Zeiss SUPRA 55VP was used for FESEM. The gas displacement-based AccuPyc 1340 Pycnometer measured density appropriately. A Micromeritics ASAP 2020 surface area analyser measured all CMTs. To determine solid-phase volume, the gadget detects pressure before and after gas transfer from a full sample chamber to an empty reference chamber. Estimated air-dried CMT density was 10–50 mg/cm^3.

Synthesis of CMTs

The cotton was uniformly placed on a glass tray and burned for 2–5 minutes. Tray-mounted thermocouples monitored combustion. Further research found carbon microtubes. Synthesis repeated under the same conditions. This combustion was done in a furnace with a vent for more air to maximise temperature. The combustion was monitored at 400–550 ºC. Rolling cotton fibres under differential aeration while burning created carbon microtubes. CMTs no longer form at 600 ºC. Self-rolling fibre sheets at the right temperatures with varied aerations will show the CMT formation mechanism during combustion at optimal conditions, and quenched and collected CMTs at 400 °C, 450 °C, 500 °C, and 550 °C were CMT_1, CMT_2, CMT_3, and CMT_4.

Density Measurement

The gas displacement-based AccuPyc 1340 Pycnometer measured density accurately. The gadget determines solid-phase volume by measuring pressure before and after transferring gas from a filled sample chamber to an empty reference chamber. Estimated air-dried CMT density is 10–50 mg/cm^3.

Determination of Surface Energy by Sorption Method

Adsorption experiments determine powder surface energy. A balance holds samples in a filter-based glass tube. How rapidly the bulk powder absorbs the testing liquid is measured by the weight increase. The Washburn equation calculates the solid-liquid moving (contact) angle in a powder bed network of capillaries and Replace the capillary radius r with a number that describes the orientation of the micro capillaries c and radius for bulk powder (eqs.-1and2), and thus, the constant replaces "r" for a powder as below:

$$\frac{l^2}{t} = \frac{r.\sigma_1.\cos\theta}{2\eta} \quad (1)$$

$$\frac{l^2}{t} = \frac{\bar{c}.r.\sigma_1.\cos\theta}{2\eta} \quad (2)$$

Bulk powder must be uniform. Mass, liquid density, and tube diameter must be used to infer the flow front due to its opacity. We know surface tension and liquid viscosity, but not advancement angle or material identity. Start with moistening liquid. Inserting a constant-slope linear segment into the time display adjusts the Washburn equation for liquid velocity variations. After acetone cleaning, rinse the containers and wipe the sample vials with cellulose. Cleaning is also assessed by water surface tension. Rinse sorption tubes with acetone and water and dry at 100 °C. Wash with hexane and dry again. Carbon microtube contact angles and capillary constants. Evaluate surface free energy (Θ, mJ/m³ or mN/m). Using Fowkes or Owens-Wendt models (eqn.-3).[17-20]

$$2\eta\frac{l}{t^2} \quad (3)$$

Equation of State
Thermal equations of state explain a system's state as a function of pressure, temperature, volume, and particles. Neumann's equation of state determines a solid's surface free energy from its contact angle with a single liquid with specified surface tension.

The Fowkes Technique
This method estimates a solid's surface free energy with test liquids. This is to determine the surface free energy's dispersive and non-dispersive components. CMT_2 surface tension is 32.4 mN/m [Disperse: 16.5, Polar: 15.9][21]

Owens-Wendt-Rabel-Kaelble Method
To calculate solid surface free energy, OWRK employs contact angle data from various liquids. Polar and dispersive surface energies are separated. Surface tension of CMT_2 is 24.8 mN/m [Disperse: 12.5 mN/m, Polar: 12.3]. [22,23]

Wu Technique [24]
Wu uses contact angle data from many liquids to determine solid surface free energy. Similar to OWRK, it differentiates dispersive and polar surface energy.

Methylene Blue Adsorption Tests
Dilute 1000 mg/L methylene blue (MB) stock solution to 10–50 mg/L for CMT adsorption. Mix 0.1 g dry CMTs with 50 mL MB in a conical flask. Continue stirring at 200 rpm at 25°C for the desired contact time (0–240 minutes). After adsorption, centrifuge or filter CMTs and detect residual MB at 665 nm with a UV-Visible spectrophotometer. The % of removal validated by the following equation:

$$\text{Percentage of dye removal} = 1 - [\text{Absorprtion at time (t)}/\text{Initial Absorbance}] \quad (4)$$

RESULTS AND DISCUSSION

Formation of CMT by Differential Aeration Mechanism
The mechanism of forming carbon microtubes begins with differential aeration, where the fiber is exposed to varying oxygen concentrations, creating regions with low and high oxygen levels. The low-oxygen areas preserve material, while higher oxygen levels cause oxidation, leading to hollowing at the core. Thermal and oxidative stresses cause the fiber to roll into a cylindrical shape, shown in Fig.-1. This rolled fiber is then subjected to pyrolysis at 400 °C to 450 °C in an air environment, where thermal decomposition stabilizes the hollow structure, ultimately transforming the material into carbon microtubes with a cylindrical morphology.

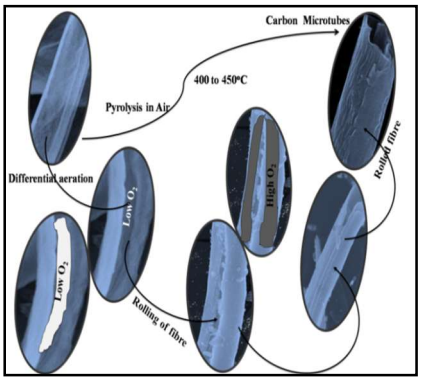

Fig.-1: The suggested CMT Formation Process by the Differential Aeration Mechanism

Contact Angle and Surface Energy Measurements
Generally, CMTs cannot determine surface energy. CMT surface energy via capillary action or sorption. CMT surface free energy was calculated using the Equation of state, Fowkes, Owens-Wendt-Rabel-Kaelble, and Wu models. Estimated air-dried carbon microtube density is 10–50 mg/cm^3. The average surface energy of CMT_2 was 22–24 mN/m. The MWCNT and CNS surface energies are similar at this

range. This shows that CMT_2 is hydrophobic and disperses better in moderately polar liquids. The surface energy / Surface Tension (mN/m) for CMT_2 was 16.5, 22.5, 13.2, and 35.9 for solid/liquid names (CMT/n-Hexane, Dichloromethane, Ethanol, and Water). CMTs are valuable as innovative adsorbent materials for removing harmful metals, chemicals, and colours from the environment due to their advanced characteristics. The average CMT_2 surface energy is 22.1 mN/m. The CMT_2 surface tension is 24.4 mN/m [Disperse 14.4, Polar 10.0]. The surface energy of CMT_2 in different solvents shows their interaction. The CMT_2 interacts most with ethanol (13.2 mN/m), indicating good compatibility due to its mild polarity and hydrogen-bonding. Due to its hydrophobicity, CMT interacts well with n-hexane (16.5 mN/m). Since dichloromethane is significantly more polar, its interaction is modest (22.5 mN/m). The maximum surface tension with water (35.9 mN/m) suggests poor interaction, indicating CMT's incompatibility with strongly polar solvents.

FESEM Analysis

The FESEM image shows a sheet-like structure and outer diameter in the micron range from 2 to 5 microns, and the length of tubes in the millimeter and provide in Fig.-2.

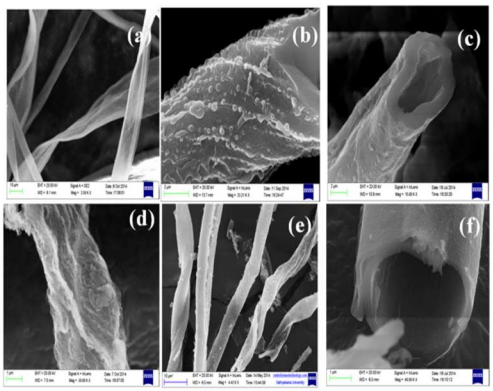

Fig.-2: FESEM Images of (a) Cotton Fiber, (b) CMT_2, (c) CMT_3 and (d) CMT_4, (e) CMT_1 (f) CMT_2

The Raman Spectra Analysis and Particle Size Distribution studies

The Raman spectra of CMT_1, CMT_2, CMT_3, and CMT_4 were provided in Fig.-3(i). The peaks observed at 1585 cm^{-1} and 1328 cm^{-1} are corresponds to the characteristic E_{2g} and D modes, respectively. The G and D are attributed to disordered carbon atoms of CMTs. All show the same Raman modes of vibrations. From Fig.-3(ii), the CILAS 1180 was used to measure particle sizes, while significance was applied. The amount of CMTs dispersed in ethanol ranged from 0.1 g for particles under 1 µm to 5.0 g for particles exceeding 400 µm. An ultrasonic vibrator prevented clumping during analysis. As the suspension passed through, a laser beam and detector measured particle size distribution and fraction weight %. Figure-3(ii) shows a histogram. An average diameter of 16 µm was measured, along with important particle size metrics including D10 = 5 µm, D50 < 10 µm, and D80 = 20 µm

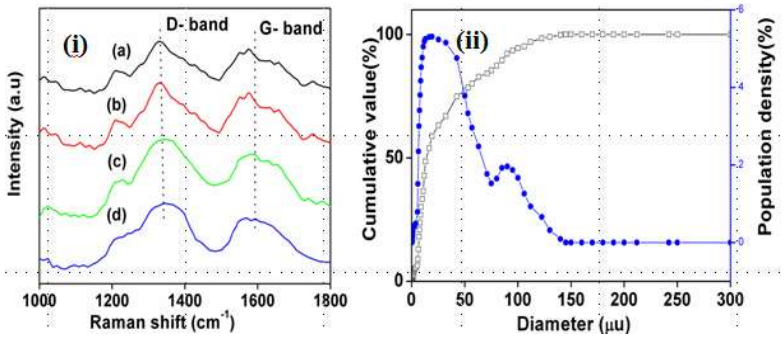

Fig.-3: (i and ii) Raman Spectrum of the (a) CMT_1, (b) CMT_2, (c) CMT_3, and (d) CMT_4. and (ii). Particle Size Distribution of the CMT_2 in Ethanol medium

XRD and XPS Analysis

The XRD patterns of CMT_1, CMT_2, CMT_3, and CMT_4 are provided in Fig.-4 (i). The diffraction two peaks and 2θ values at 25.9° and 43.5° for the (0 0 2) and (1 0 0) diffraction, respectively. The broadening and lowering peak intensity observed for CMT_4, even for CMT_3. This is due to a decrease in the crystallinity of the CMTs at higher temperatures. The XRD studies indicate that the graphitic carbon structure of carbon microtubules. The XPS analysis for the CMT_2 was recorded, and traces are provided in Fig.-4(ii). The surface chemical state and oxidation sate, valences, and purity of the CMTs can be detected by XPS surface analysis.[6] The survey graph indicate that carbon 1s peak at 285.4 eV for the CMT_2. Hence, XPS analysis suggests the purity of the CMTs.

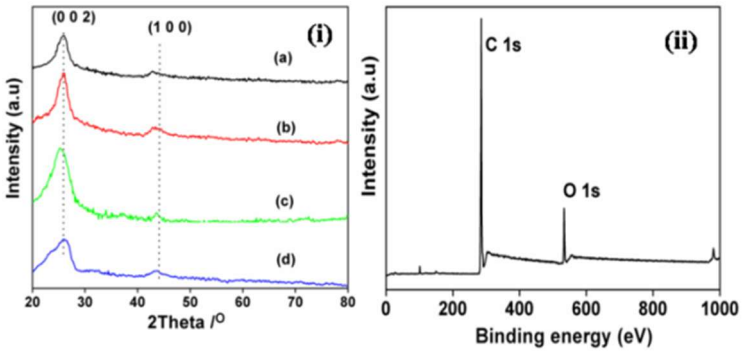

Fig.-4: (i) Powder XRD Patterns of the (a) CMT_1, (b) CMT_2, (c) CMT_3, and (d) CMT_4, (ii) XPS Survey Spectrum of CMT_2

Methylene Blue dye Absorption studies

Photocatalytic adsorption studies carried out by and calculated by Eq.1 break down dyes with visible light and a catalyst. Light stimulates the catalyst, forming electron-hole pairs. These create ROS-like hydroxyl radicals with oxygen and water. ROS degrades dyes into safer compounds. Catalyst, light, dye, and reactive oxygen radical-ions (OH^{-}) affect efficiency.[6,23] This study examined the photocatalytic decolorisation of methylene blue dye using four catalysts provided in the Fig.-4: CMT_1, CMT_2, CMT_3, and CMT_4. The findings of each catalyst's decolorisation efficiency are shown in Fig.-5 and Fig.-6.

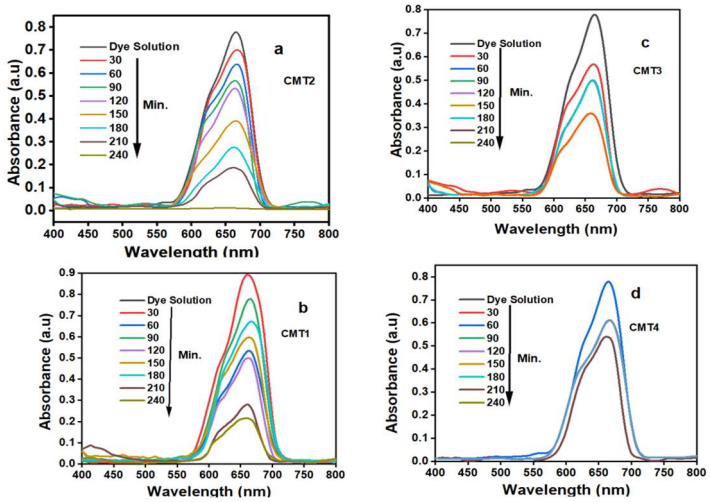

Fig.-5: (a) CMT_2 ;(b) CMT_1 ;(c) CMT_3 and (d) CMT_4 MB Degradation Profile for the Catalysts with Time

These studies CMT_1 had a decolonization percentage of 75%, CMT_2 100%, CMT_3 63.75%, and CMT_4 38.75%.The testing results show that CMT_2 decolorises methylene blue dye best. Decolonization efficiency was good for CMT_1 and modest for CMT_3. The least effective catalyst was CMT_4, which had the lowest decolorisation activity. Four Methylene Blue (MB) dye degradation catalysts were examined. Reducing

absorbance with time indicates dye degradation in graphs. CMT_2 had the fastest absorbance decline (most effective), followed by CMT_3, CMT_1, and CMT_4. CMT_2 and CMT_1 have a high surface area, but CMT_3 and CMT_4 have a low surface area and morphology that confirms tubular structure loss, which may be the main reason MB dye is removed. CMT_2 has superior adsorption based on surface energy. This work shows that CMTs can remove pollutants by solar/visible-light-driven photocatalysis, supporting clean water and sustainable energy strategies and Sustainable Development Goals 6 and 7. Figure-6 shows CMT_1, CMT_2, CMT_3, and CMT_4 decolorisation over time. At 240 minutes, CMT_1 regularly removes 60% colour. Though slower than CMT_3, CMT_2 outperforms the others after 90 minutes and removes practically all colour after 240 minutes. CMT_3 eliminates things fastest (60%) after 90 minutes, but it plateaus at 70% after 240 minutes, limiting its expansion. Poorest CMT_4 decolorises slowly (30% at 240 minutes). Most efficient is CMT_2 (100%), followed by CMT_1 (75%), CMT_3 (63.75%), and CMT_4 (38%). CMT_2 removes colour best, CMT_3 begins quickly but stops, CMT_1 is medium, and CMT_4 is least effective.

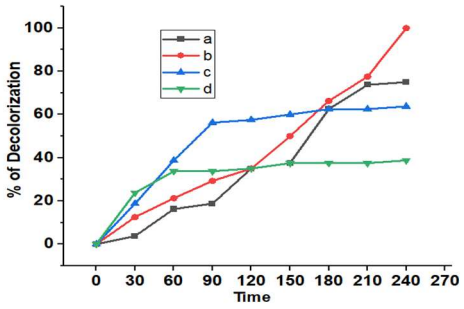

Fig.-6: Plot between % conversion vs. Time

CONCLUSION

The study successfully demonstrated an innovative and cost-effective approach to producing CMTs under ambient conditions. The differential aeration process was proven to be the key to the creation of these materials by the physico-chemical characterization. The visible-light-driven photocatalysis in CMTs removes contaminants, promoting clean water, sustainable energy, and Sustainable Development Goals 6 and 7. The surface analyses and microscopic analyses suggest that CMTs hold significant potential for applications in catalysis, sustainable energy, and environmental technologies. Photocatalytic experiments on methylene blue dye revealed that CMT_2 exhibited superior performance, achieving complete decolorization (100%). CMT_1 also showed commendable efficiency with a 75% decolorization rate, followed by CMT_3 at 63.75%. In contrast, CMT_4 was the least effective, with a decolorization efficiency of only 38.75%. Estimated air-dried CMT density is 10–50 mg/cm^3. These findings indicate that CMT_2 is the most promising catalyst among those tested for dye degradation under the experimental conditions, underscoring its potential for advanced photocatalytic applications.

ACKNOWLEDGMENTS

All authors are thankful to the Management of Sathyabama Institute of Science and Technology (Deemed to be University), Chennai–600119, for their consistent support and for providing the necessary facilities to carry out this work.

CONFLICT OF INTERESTS

It is not admitted by the writers that there is no prejudice or conflict of interest.

AUTHOR CONTRIBUTIONS

The present work is related to *SDG-6: Clean Water and Sanitation*. All the authors contributed significantly to this manuscript, participated in reviewing/editing and approved the final draft for publication. The research profile of the authors can be verified from their ORCID ids, given below:

A. Sunitha https://orcid.org/0009-0007-2960-814X
K. Chennakesavulu https://orcid.org/0000-0002-3415-1865
G. Ramanjaneya Reddy https://orcid.org/0000-0001-5509-0873

REFERENCES

1. M. Anwar, F. Muhammad, B. Akhtar, *Journal of Drug Delivery Science and Technology*, **64**, 102638(2021), https://doi.org/10.1016/j.jddst.2021.102638
2. C. Wang, Z.-X. Guo, S. Fu, W. Wu, D. Zhu, *Progress in Polymer Science*, **29**, 1079(2004), https://doi.org/10.1016/j.progpolymsci.2004.08.001
3. M. Richter, T. Heumüller, G. J. Matt, W. Heiss, C. J. Brabec, *Advanced Energy Materials*, **7,** 1601574(2017), https://doi.org/10.1002/aenm.201601574
4. K. Shirvanimoghaddam, B. Czech, A. E. Wiacek, W. Cwikła-Bundyra, M. Naebe, *Chemical Engineering Journal*, **361**, 1605(2019), https://doi.org/10.1016/j.cej.2018.11.157
5. H. Yang, J. Yin, J. Yang, S. Tang, W. Zhang, G. Yang, *Nano Energy*, **125**, 109591(2024), https://doi.org/10.1016/j.nanoen.2024.109591
6. J. Wu, X. Zhang, Z. Zhao, J. Wu, J. Wang, J. Wang, *Materials Letters*, **261**, 127079(2020), https://doi.org/10.1016/j.matlet.2019.127079
7. K. Chennakesavulu, G. R. Reddy, *RSC Advances*, **5**, 56391(2015). https://doi.org/10.1039/C5RA06812F
8. https://unstats.un.org/sdgs/report/2024/
9. H. Peng, Y. T. Zhu, D. E. Peterson, Q. Jia, *Carbon microtubes and methods of making the same*, US Patent US7959889B2(2011).
10. R. Bacon, *Journal of Applied Physics*, **31**, 283(1960), https://doi.org/10.1063/1.1735559
11. C. C. Han, J. T. Lee, R. W. Yang, H. Chang, C. H. Han, *Chemistry of Materials*, **11**, 1806(1999), https://doi.org/10.1021/cm990032p
12. S. Paul, S. K. Samdarshi, *New Carbon Materials*, **25**, 321(2010), https://doi.org/10.1016/S1872-5805(09)60036-6
13. E. Kanagaraj, P. Mahalingam, R. Siddharthan, P. Sivakumar, *Rasayan Journal of Chemistry*, **14(4)**, 2311(2021), https://doi.org/10.31788/RJC.2021.1446485
14. H. B. Haanstra, W. F. Knippenberg, G. Verspui, *Journal of Crystal Growth*, **16**, 71(1972), https://doi.org/10.1016/0022-0248(72)90091-7
15. H. H. Nersisyan, T. H. Lee, K. H. Lee, D. Y. Maeng, J. H. Lee, *Materials Letters*, **107**, 79(2013), https://doi.org/10.1016/j.matlet.2013.05.102
16. S. Sivaprakash, S. K. Krishna, *Rasayan Journal of Chemistry*, **12**, 2166(2019), https://doi.org/10.31788/RJC.2019.1245181
17. X. G. Chen, S. S. Lv, P. P. Zhang, J. P. Cheng, S. T. Liu, Y. Ye, *Journal of Magnetism and Magnetic Materials*, **324**, 1745(2012), https://doi.org/10.1016/j.jmmm.2011.12.043
18. K. Kumar, B. Nandan, P. Formanek, M. Stamm, *Journal of Materials Chemistry*, **21**, 10813(2011), https://doi.org/10.1039/C1JM11258A
19. F. M. Fowkes, *Industrial and Engineering Chemistry*, **56**, 40(1964), https://doi.org/10.1021/ie50660a008
20. D. K. Owens, R. C. Wendt, *Journal of Applied Polymer Science*, **13**, 1741(1969), https://doi.org/10.1002/app.1969.07013081
21. K. Chennakesavulu, G. B. Raju, S. Prabhakar, *Journal of Physical Organic Chemistry*, **23**, 723(2010), https://doi.org/10.1002/poc.1641
22. D. H. Kaelble, *The Journal of Adhesion*, **2**, 66(1970), https://doi.org/10.1080/0021846708544582
23. S. Wu, *The Journal of Adhesion*, **5**, 39(1973), https://doi.org/10.1080/00218467308078437
24. M. M. Reddy, G. R. Reddy, K. Chennakesavulu, E. Sundaravadivel, S. S. Prasath, A. M. Rabel, J. Sreeramulu, *Journal of Porous Materials*, **24(1)**,149(2017), https://doi.org/10.1007/s10934-016-0247-3

[RJC-9380/2025]